

632. Transient analysis of drum brake squeal with binary flutter and negative friction-velocity instability mechanisms

Choe-Yung TEOH, Zaidi Mohd RIPIN*

School of Mechanical Engineering, Universiti Sains Malaysia,
14300 Nibong Tebal, Pulau Pinang, Malaysia.

*Tel.: 604-5941024;

Fax: 604-5941025.

E-mail: mezaidi@eng.usm.my

(Received 10 February 2011; accepted 15 May 2011)

Abstract. A two degree-of-freedom model of a drum brake system is developed to investigate the criteria for unstable condition under friction-induced vibration instability mechanisms of both flutter instability and negative friction-velocity instability. This model considers the drum as the main component that is subjected to the friction-induced vibration. The influences of the friction coefficient, normal load, sliding velocity, contact stiffness, damping coefficient and the location of centre of pressure on the shoes on the instability of the system are investigated using transient analysis. The results indicate that the minimal model displays all the characteristics of the unstable system comparable to the previously published experimental and finite element modeling results.

Keywords: minimal model, self-excited friction induced vibration, drum brake squeal, flutter instability, negative damping.

Nomenclature

Symbol	Notation	Initial value
c_1	Damping coefficient of drum in horizontal x -direction	218 Ns/m
c_2	Damping coefficient of drum in vertical y -direction	212 Ns/m
k_1	Spring stiffness of drum in horizontal (x) direction	19×10^6 N/m
k_2	Spring stiffness of drum in vertical (y) direction	18×10^6 N/m
k_3	Contact stiffness between shoe 1 and drum	19×10^7 N/m
k_4	Contact stiffness between shoe 2 and drum	11×10^7 N/m
m	Mass of the brake drum	1 kg
N	Normal load applied from hydraulic cylinder on shoes	1000 N
V_B	Velocity of belt / velocity of vehicle	0.2 m/s
x	Vibration displacement of drum in x direction	-
\dot{x}	Vibration velocity of drum in x direction	-
\ddot{x}	Vibration acceleration of drum in x direction	-
y	Vibration displacement of drum in y direction	-
\dot{y}	Vibration velocity of drum in y direction	-
\ddot{y}	Vibration acceleration of drum in y direction	-
η	Loss factor of brake drum	0.02
θ_1	Location of center of pressure of shoe 1	35°
θ_2	Location of center of pressure of shoe 2	115°
μ	Friction coefficient between shoes and the drum	0.30

Introduction

Brake squeal is a type of self-excited friction induced vibration and has been studied using various methods including the finite element method [1-3], analytical [4-7] and the experimental approach [8-12]. In general there are four different excitation mechanisms that can be used to model the brake as friction-excited vibration which include the velocity dependent friction coefficient that leads to negative damping [13-14], mode-coupling [14-15], sprag-slip and follower force nature of the friction force [16]. Guan et. al [17] studied the brake squeal using feed-in energy analysis, where the calculation method of feed-in energy method was derived and parameters sensitivity study carried out. Haverkamp and Koopmann [18] studied the drum brake squeal using Acoustic Quality Control where the drum brake shoe was considered as the main source of squeal.

In general, drum brake squeal is modeled as stability problem of self-excited vibration with the stability measured by the real part of the complex eigenvalue analysis of the linear system. In such case the complex eigenvalue problem is obtained from the equation of motion of the system and the forcing function due to the friction interface is usually posed as part of the system stiffness (usually represented as contact stiffness) relating the normal displacement to the variation of the normal force which in turn is related to the friction force based on the Amonton's law [19-20]. Experimental data verifying this approach can be found in Okamura's work, where the squeal propensity of disc brake can be related to the real part of the eigenvalue of the system [21]. The complex eigenvalue technique can be considered as the most popular approach of modeling brake squeal. The main mechanism for this type of instability is also known as binary flutter type instability due to the convergence of two separate modes to become a common mode at one frequency which has phase relationship enabling efficient energy transfer [22]. Stability of the drum brake system is studied usually as a function of the design parameters, which include the lining friction coefficient, lining stiffness, brake actuation system stiffness and the geometry of the shoes and rotor [1, 8, 23, 24].

Another mechanism for friction-excited vibration is due to the friction characteristics of the brake shoe-rotor pair when the friction coefficient decreases with the velocity or negative friction-velocity gradient, which is also known as negative damping effect. This effect has been used by many researchers namely Ouyang et al. [25], Capone et al. [26] and Shin et al. [13]. These models were able to show that squeal manifests itself as limit cycle and the squeal propensity can be measured by the size of the limit cycles. As such the effect of the brake design parameters can be evaluated. Of particular interests is the result from Shin et al. [13], where increase of damping to a particular component only may be detrimental to the system stability. Hoffmann et al. [27] showed that harmonic balance and averaging technique can be used to determine the limit cycles of unstable system and this is particularly useful for stability comparison.

Minimal model is defined as a system with minimum degree of freedom (usually two degree-of-freedom) to represent a dynamic vibration system. There have been several minimal models developed for friction induced vibration and disc brake squeal [13, 22, 27, 28]. Von Wagner et al. [28] used a minimal model to describe the basic behavior of disk brake squeal, where the vibration of the disk and radius of brake disc were taken into account. Hoffmann et al. [27] set up a minimal model to represent mode-coupling friction induced instability with Coulomb-type frictional nonlinearity using harmonic balance approaches. Hashemi-Dehkordi et al. [29] used Active Force Control (AFC) on a minimal disc brake model to reduce friction induced vibration and reduce brake squeal with PID controller. They stated that PID controller with AFC is more effective in reduction of vibration compared to pure PID controller. Hoffmann [16] has shown that high-frequency dither can be used to bring stability back to friction-excited vibration for flutter type instability. From the literature reviewed, the model of drum brake with both instability mechanisms has not been developed and analyzed before. Such

model is necessary in order to analyze squeal under deceleration, which typically occurs during stopping.

The drum brake system is different from the disc brake system. The development of minimal model of drum brake must capture the essence of the drum brake system and have physical relationship to the drum brake geometry. Active control on drum brake is important since it is one of the many ways available to eliminate squeal. In such application minimal model is very useful since model of large degrees of freedom (typical of finite element model) is not amenable to time-domain analysis due to the large computational effort required. In this paper a minimal model of a drum brake is developed, which is subjected to two instability mechanisms of both the flutter type instability and negative friction-velocity gradient are used to assess the performance of the model. Drum brake squeal in general occurs during stopping and experience have shown that buses and lorries suffer squeal at the final phase of the stopping. In such cases, the vehicle is decelerating and both the flutter type instability and the negative friction-velocity gradient are active. In this paper, the drum brake model employs both binary flutter and negative friction-velocity mechanism to simulate this condition. The peculiar aspects of drum brake are listed and how these are incorporated in the minimal model is discussed. Stability analysis is carried out using transient analysis since the model is nonlinear with velocity-dependant friction coefficient and to take into account the deceleration motion of the drum during stopping.

Minimal model of the drum brake

The drum brake system is represented by a two degree-of-freedom system as shown in Fig. 1. Only in-plane vibration is considered since diametral modes are the main source of unstable vibration, thus x-y coordinates are used. This model consists of a single mass sliding on two conveyor belts representing the rotating drum sliding on the brake shoes. The x-y motion of mass, m represented the motion of the drum in horizontal and vertical direction respectively. The spring k_1 , k_2 and damper c_1 , c_2 represented the drum stiffness and damping properties respectively. Meanwhile, the contact stiffness of k_3 and k_4 represent the contact interface of the leading and trailing shoes respectively. In this case the brake shoes are not represented explicitly. The shoes-rotor interaction is limited to the contact stiffness only. Both conveyor belts represent the sliding condition between drum and the brake shoes. The friction coefficient μ can modeled both the velocity independent and velocity dependant friction coefficient to determine their effect on the stability of the system. The center of contact pressure by the hydraulic press from the shoes to the drum can be shifted along the drum surface with the change of type of drum brake (leading/trailing or twin leading), angle of the applied load, shape of the shoes and the pivot point of the shoes. The locations of the center of contact pressure of the leading and trailing shoes in this model are represented by θ_1 and θ_2 respectively. This effect is important since the shoes will wear throughout the operation, which affects the contact pressure distribution of the shoes on the drum. Sliding speed, V_B for both conveyor belts is the same since both of them represent the rotation speed of the drum. Thus, this model only shows the effect dominated by the drum brake dynamics. Based on this model, the influence of the friction coefficient, the normal load, location of the center of pressure of the shoes to the drum and the sliding speed can be investigated for both instability mechanisms.

Equation of motion

The contact stiffness k_3 and k_4 will contribute to the stiffness in x and y direction depending on the location of center of pressure (θ_1 , θ_2). The equation of motion of the system can be written as below in a matrix form:

$$\begin{aligned}
 & \begin{bmatrix} m & 0 \\ 0 & m \end{bmatrix} \begin{pmatrix} \ddot{x} \\ \ddot{y} \end{pmatrix} + \begin{bmatrix} c_1 & 0 \\ 0 & c_2 \end{bmatrix} \begin{pmatrix} \dot{x} \\ \dot{y} \end{pmatrix} + \begin{bmatrix} k_{11} & k_{12} \\ k_{21} & k_{22} \end{bmatrix} \begin{pmatrix} x \\ y \end{pmatrix} \\
 & = \begin{pmatrix} N_1 \sin \theta_1 - N_2 \sin \theta_2 + \mu k_3 x \sin^2 \theta_1 \operatorname{sgn}(V_B \cos \theta_1 - \dot{x}) - \mu k_4 x \sin^2 \theta_2 \operatorname{sgn}(V_B \cos \theta_2 - \dot{x}) \\ -N_1 \cos \theta_1 + N_2 \cos \theta_2 - \mu k_3 y \cos^2 \theta_1 \operatorname{sgn}(V_B \sin \theta_1 - \dot{y}) + \mu k_4 y \cos^2 \theta_2 \operatorname{sgn}(V_B \sin \theta_2 - \dot{y}) \end{pmatrix} \quad (1)
 \end{aligned}$$

where the coefficients of the stiffness matrix can be obtained from elementary considerations as:

$$\begin{aligned}
 k_{11} &= k_1 + k_3 \sin^2 \theta_1 + k_4 \sin^2 \theta_2 \\
 k_{12} &= k_{21} = k_3 \sin \theta_1 \cos \theta_1 + k_4 \sin \theta_2 \cos \theta_2 \\
 k_{22} &= k_2 + k_3 \cos^2 \theta_1 + k_4 \cos^2 \theta_2
 \end{aligned}$$

and the velocity dependant friction coefficient, μ :

$$\mu = \mu_0 - \alpha |V_B \cos \theta - \dot{x}| \quad \text{or} \quad \mu_0 - \alpha |V_B \sin \theta - \dot{y}| \quad (2)$$

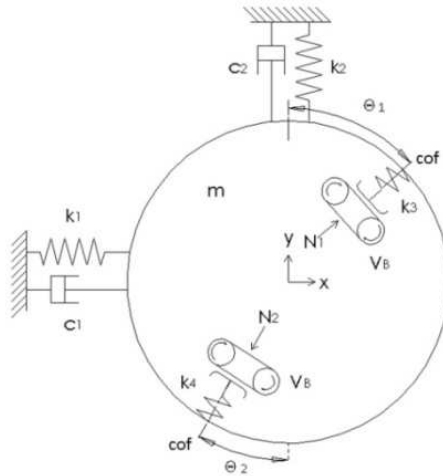


Fig. 1. Minimal model of the drum brake

The friction coefficient varies with the sliding velocity between the drum and the brake shoe. The terms $|V_B \cos \theta - \dot{x}|$ and $|V_B \sin \theta - \dot{y}|$ represent the components of sliding velocity between the drum and the brake shoe in x-axis and y-axis respectively which considers the vibration's velocity of the drum.

In force matrix, the term $N_1 \sin \theta_1 - N_2 \sin \theta_2$ represent the component of external force exerted on the drum from the hydraulic press through brake shoe in horizontal direction (x-axis). Meanwhile, the term $-N_1 \cos \theta_1 + N_2 \cos \theta_2$ represents the component of external force in vertical direction (y-axis). The terms $\mu k_3 x \sin^2 \theta_1 - \mu k_4 x \sin^2 \theta_2$ and $-\mu k_3 y \cos^2 \theta_1 + \mu k_4 y \cos^2 \theta_2$ represent the components of frictional force in x-axis and y-axis respectively. The frictional forces are not directly due to the normal force, N , thus it more accurately represents by function of frictional force, μ and spring compression displacement, $k_3 x \sin^2 \theta_1 - \mu k_4 x \sin^2 \theta_2$ (x-axis) or $-k_3 y \cos^2 \theta_1 + k_4 y \cos^2 \theta_2$ (y-axis). The sign functions, $\operatorname{sgn}(V_B \cos \theta_1 - \dot{x})$, $\operatorname{sgn}(V_B \cos \theta_2 - \dot{x})$, $\operatorname{sgn}(V_B \sin \theta_1 - \dot{y})$ and $\operatorname{sgn}(V_B \sin \theta_2 - \dot{y})$ represent the direction of the frictional force. The direction of the

frictional forces varies with the change of vibrational velocity of the drum while conveyor belts speed remains constant. When the vibration velocity of the drum is greater than the conveyor belts speed, friction force will change direction.

By rearranging Eq. (1), the equation of motion in matrix form becomes:

$$\begin{bmatrix} m & 0 \\ 0 & m \end{bmatrix} \begin{pmatrix} \ddot{x} \\ \ddot{y} \end{pmatrix} + \begin{bmatrix} c_{11} & 0 \\ 0 & c_{22} \end{bmatrix} \begin{pmatrix} \dot{x} \\ \dot{y} \end{pmatrix} + \begin{bmatrix} k_{11} & k_{12} \\ k_{21} & k_{22} \end{bmatrix} \begin{pmatrix} x \\ y \end{pmatrix} = \begin{pmatrix} N_1 \sin \theta_1 - N_2 \sin \theta_2 \\ -N_1 \cos \theta_1 + N_2 \cos \theta_2 \end{pmatrix} \quad (3)$$

where:

$$c_{11} = c_1 \pm \alpha N (\cos^2 \theta_1 + \cos^2 \theta_2)$$

$$c_{22} = c_2 \pm \alpha N (\sin^2 \theta_1 - \sin^2 \theta_2)$$

$$k_{11} = k_1 + k_3 \sin^2 \theta_1 + k_4 \sin^2 \theta_2$$

$$k_{12} = \pm k_3 (\alpha V_B \cos^3 \theta_1 - \mu_o \cos^2 \theta_1 + \sin \theta_1 \cos \theta_1) \pm k_4 (-\alpha V_B \cos^3 \theta_2 + \mu_o \cos^2 \theta_2 + \sin \theta_2 \cos \theta_2)$$

$$k_{21} = \pm k_3 (-\alpha V_B \sin^3 \theta_1 + \mu_o \sin^2 \theta_1 + \sin \theta_1 \cos \theta_1) \pm k_4 (\alpha V_B \sin^3 \theta_2 - \mu_o \sin^2 \theta_2 + \sin \theta_2 \cos \theta_2)$$

$$k_{22} = k_2 + k_3 \cos^2 \theta_1 + k_4 \cos^2 \theta_2$$

In this matrix form it is obviously shown that the damping matrix and stiffness matrix will become unsymmetrical or negative with the change of values of the parameters. This unsymmetry or negative damping matrix or stiffness matrix will lead to the unstable vibration, which results in the brake squeal. The \pm sign in the equation is dependent on the direction of the relative sliding velocity between drum and the brake shoes. When the vibration velocity of the drum is greater than the drum rotating speed (speed of conveyor belts), the frictional force will change direction.

For the velocity dependant friction coefficient, it is assumed to vary linearly with the velocity as shown in Fig. 2. In this figure the value of gradient, α is based on Shin et al. [13]. Both flutter instability and negative friction-velocity mechanisms will be excited when considering both velocity dependant friction coefficient and also the contact stiffness between the drum and brake shoes.

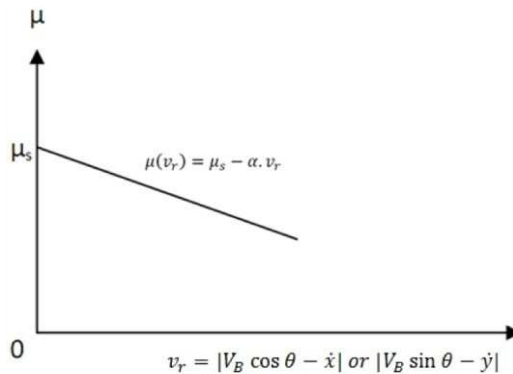


Fig. 2. Velocity dependant friction coefficient

Numerical analysis

The equation of motion Eq. (1) is solved in numerical analysis using Bogacki-Shampine method [30]. Bogacki-Shampine method is one of the Runge-Kutta methods to solve ordinary differential equations. This method is chosen rather than other numerical methods such as Dormand-Prince, Adams, Mod. Rosenbrock or Trapezoidal method because of its suitability to the second-order equation of motion, Eq. (1). Bogacki-Shampine method uses approximately

three function evaluations per step. It has an embedded second-order method, which can be used to implement adaptive step size. Thus, it is suitable for second-order equation as Eq. (1).

The transient analysis is carried out for a period of 0.05 seconds. Within this period, the stability of the system can be observed clearly. The spring stiffness and mass value used in this study are taken from previous researchers [1, 4]. The damping coefficients, c are calculated from value of m and k with loss factor, η of 0.02. The initial values of the parameters are given as in nomenclature.

The friction coefficient, μ values are from 0.1 to 0.5. The load, N varies from 5000 N to 25000 N and the speed, V_B varies from 1 m s⁻¹ to 0.05 m s⁻¹ with 3 m s⁻² deceleration. In this model, the friction-velocity characteristics can be activated when required. The output of the simulation is presented in time-series and phase-plane. This is important since the system is nonlinear due to the velocity dependant friction coefficient. The relative instability can be measured from the limit cycle displacement. The frequency range being investigated is between 0 Hz to 5000 Hz since most of the drum brake squeals are observed in this range of frequencies.

Results and discussion

The results of the influence of various parameters on the instability of drum brake squeal and the response are shown using time response, frequency response function and phase-plane. Since the behaviors of the vibration in horizontal and vertical direction are almost the same, only the results for x direction are presented.

Effect of friction coefficient, μ

Fig. 3 and Fig. 4 indicate the effect of initial friction coefficient for the combined instability mechanisms. The study of effect of friction coefficient on the stability of the drum brake system is carried out in the range of 0.1 to 0.5 while other baseline values remain unchanged. Based on the results shown in Fig. 3, the system is stable for $\mu=0.10$ to $\mu=0.39$ and the amplitude of the drum vibration decreases with time. The displacement graph reveals beating phenomena at $\mu=0.39$. The beating amplitude increases with time until it transform to instability at $\mu=0.40$, where the vibration amplitude of the drum increases with time, which indicates unstable vibration. When μ is increased from 0.40 to 0.50, the amplitude of the limit cycle vibration also increases from 0.11 mm to 0.20 mm. When the value of μ is increased over the value of 0.40, the energy feed into the system due to the friction coefficient is sufficient to excite unstable vibration.

As in Eq. (1), the degree of unsymmetry of stiffness matrix due to the friction coefficient increase with the increasing of friction coefficient until it excites the unstable vibration when the value of μ exceeds 0.40. The natural frequencies at $\mu=0.1$ are 11240 rad s⁻¹ and 14570 rad s⁻¹ respectively. At $\mu=0.39$, the results shows an interesting beating phenomena as the two initially separated frequencies began to get closer to each other with frequency differences of only 560 rad s⁻¹. At the onset of instability at $\mu=0.40$ the coalescence is complete at 13140 rad s⁻¹ with limit cycle vibration of 0.11 mm.

The beating phenomenon observed in Fig. 3 is similar to the observation made by Hoffmann et al. [10], where mode coupling was observed to cause beating phenomenon before the onset of instability. When μ increases from 0.40 to 0.50 the unstable mode frequency decreases further to 12190 rad s⁻¹ with increase in the value of the limit cycle displacement to 0.20 mm. The decreasing of the frequency of the excited mode is due to the decrease of amplitude of stiffness matrix with increase of friction coefficient as provided in Eq. (3). The values of k_{12} and k_{21} decrease with the increase of friction coefficient. The coalescence of the two modes of the drum with increasing μ is shown by the two initially separated frequencies converged at $\mu=0.40$ and remain together afterward. This is an indication of mode coupling, which is the primary mechanism of instability for the binary flutter. The instability of the system increases with μ

can be explained based on Eq. (1). Increase in μ will increase the degree of unsymmetry of the stiffness matrix which causes the unstable vibration. These observations are similar to other published results [1, 4, 5, 7, 8, 12, 19].

The negative friction-velocity instability had not been excited with the changing of friction coefficient. Based on Eq. (3), the damping matrix in the equation of motion will not be affected with the change of friction coefficient.

The effect of negative damping only increases the critical value of friction coefficient but does not influence the frequency and also the amplitude of the unstable mode. Fig. 5 shows the coalescence of the two modes of the drum with increasing μ where two initially separated frequencies converges at $\mu=0.40$ and remain together afterward confirming the binary flutter mechanism on the instability mechanism here.

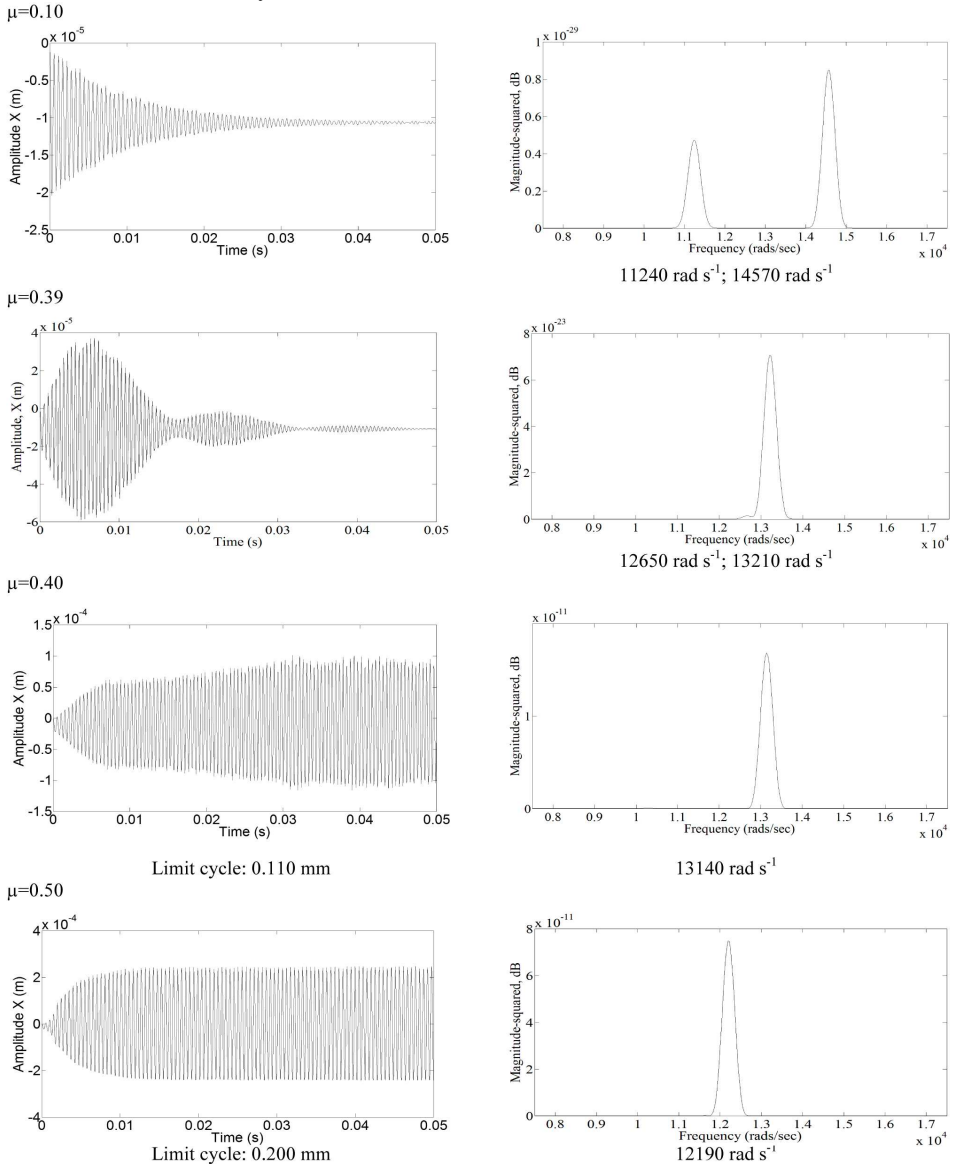


Fig. 3. Time series and frequency responses for various values of friction coefficient

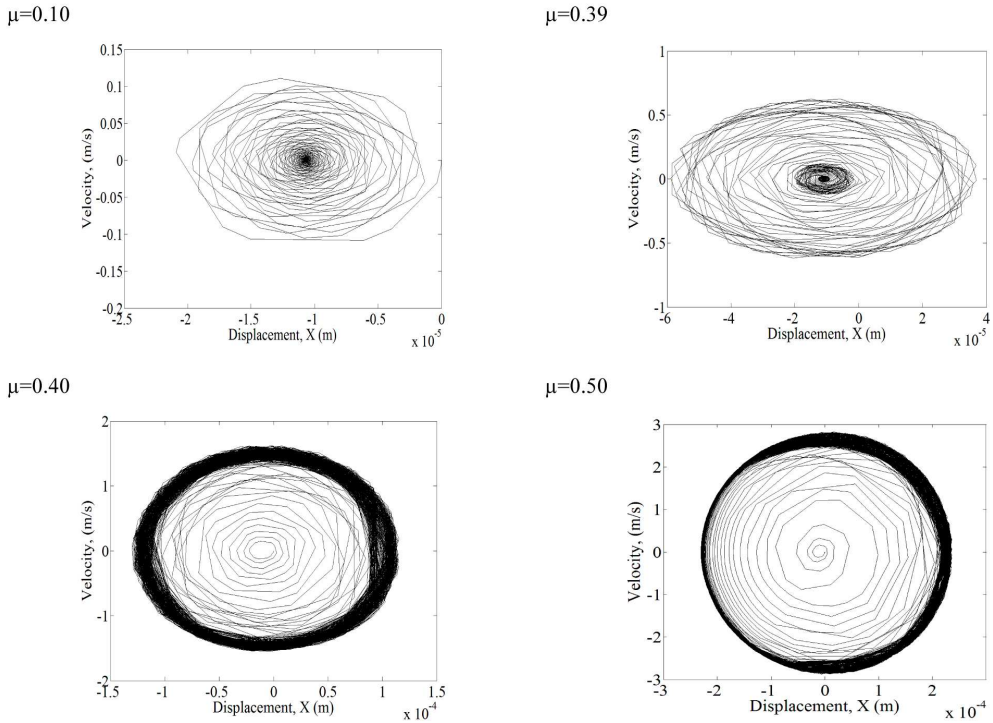


Fig. 4. Phase-plane for various values of friction coefficient

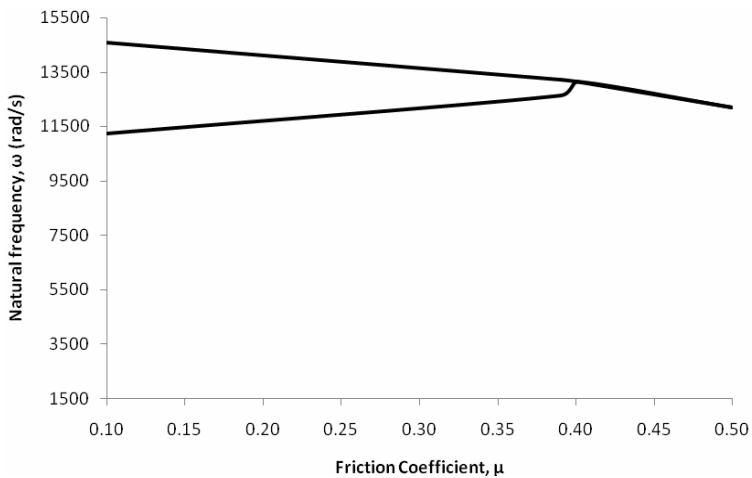


Fig. 5. Variation of frequencies with μ for binary flutter mechanism

Effect of normal load, N

In the study of the normal load, N is varied from 5 kN to 25 kN to represent the normal load applied on the shoes. Figs. 6-7 illustrate the progression of the load and each individual load response. In this case, instability begins at $N=15$ kN, which causes one of the two initially separated frequencies to become unstable for the frequency of 11790 rad s^{-1} and the other frequency of 14060 rad s^{-1} to be stable. When the load is increased beyond 15 kN, the system becomes unstable. At the load of 15 kN, the negative damping effect overcomes the system

damping. The vibration amplitude also increases when the load is increased. The natural frequencies of the system do not combine but the negative damping effect excited one of the natural frequency that is 11790 rad s^{-1} for 15 kN. The higher natural frequency cannot be clearly observed since it is relatively small in amplitude compared to the excited lower natural frequency.

From the phase plane in Fig. 7, the locus of the circle is repeating at certain radius from the center of circle starting from load 15 kN. When the load increases, the radius of the circle also increases indicating higher level of instability. Experimental results of Ioannidis et al. [11] showed that the drum brake instability increases with the load. This observation supports the trend shown in Figs. 6-7, where the instability increases with load. The load dependant stability of the system can be explained from Eq. (1), where the amplitude of the load affect the damping matrix of the system through the term $N\alpha(\cos\theta_1 - \cos\theta_2)$ and when this is greater than the damping coefficient (c_1, c_2) the damping matrix will become negative and causes instability of the system. For normal load of 15 kN and 25 kN, although the system are unstable, the time series results shows that the vibration amplitude decrease with time for $t = 0 \text{ s}$ to $t = 0.004 \text{ s}$, after that the amplitude of the vibration only maintains at 0.16 mm. Unlike the unstable vibration excited by binary flutter instability, the amplitude of the vibration took longer time to reach its limit cycle, the negative damping due to the constant load of 25 kN is only sufficient to maintain the amplitude of the unstable vibration at 0.16 mm although it overcomes the system damping.

Effect of sliding speed, V_B

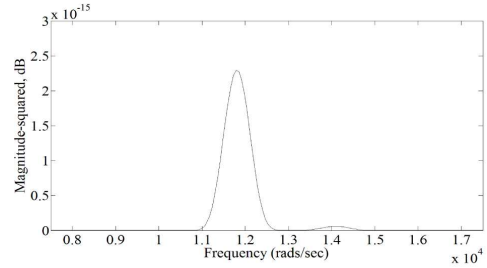
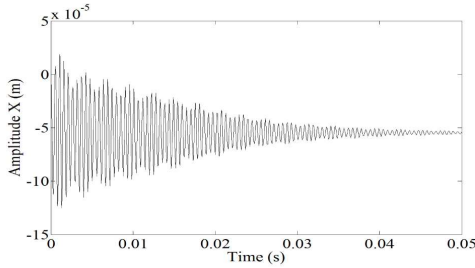
The analysis is carried out for period of 0.05 second with constant deceleration of -4 m s^{-2} . The initial speed is set to 0.2 m s^{-1} . The vehicle will stop down at $t=0.05$ second. From the time history result in Fig. 8, the amplitude of the vibration decrease with time from $t=0$ to $t=0.02$ sec with beating phenomena. This period of time is equivalent to speed 0.2 m s^{-1} to 0.12 m s^{-1} . After that, the amplitude of the vibration becomes constant from $t=0.02 \text{ s}$ to $t=0.037 \text{ s}$. This indicate that at the sliding velocity of 0.12 m s^{-1} to 0.05 m s^{-1} , the drum brake system vibrate in unstable condition where the excited vibration have sufficient energy to overcome the system damping. Finally the amplitude again decreases with time until the vibration stop where stable vibration is detected again. From the phase-plane in Fig. 8, the limit cycle for unstable vibration is 0.0045 mm . From the frequency response function in Fig. 8, the excited frequency is 11790 rad s^{-1} . The unstable vibration that is affected by the sliding speed is only excited in the range of 0.12 m s^{-1} to 0.05 m s^{-1} , and the energy of this unstable mode is only sufficient to overcome the damping of the system (zero damping) but does not magnify the vibration. The effect of sliding speed only excites one of the natural modes of the system but coupling of the modes does not occur.

Effect of center of pressure

The considered range of location of center of pressure is from 20° to 160° for both θ_1 and θ_2 . Fig. 9 indicates the unstable region for the values of the center of pressure on the drum (based on the location of leading and trailing shoes). It can be observed that the area of instability is narrow and large area of stable zone of operation can be found. Zone where θ_1 is 115° to 155° and θ_2 is 20° to 40° is prone to instability. In the actual drum brake, the contact pressure is rarely uniform as shown by Ioannidis et al. [23], where the contact occurs mostly at $\theta_1=30^\circ - 110^\circ$ and $\theta_2=30^\circ - 70^\circ$ for $\mu=0.35$. The results shown in Fig. 9 are comparable in terms of unstable mode and the value of friction coefficient. The hatched region indicated the unstable location of the drum. It demonstrates than the stability of the drum brake is dependent on location of the center of pressure. The location of center of pressure on the drum will vary with the change of mounting geometry of the shoes, wearing condition of the shoe lining, geometry

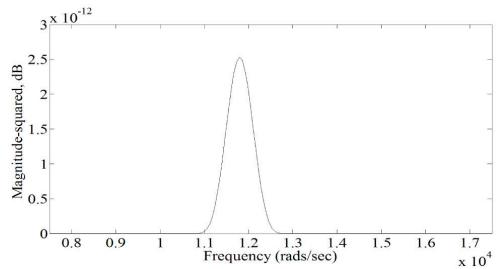
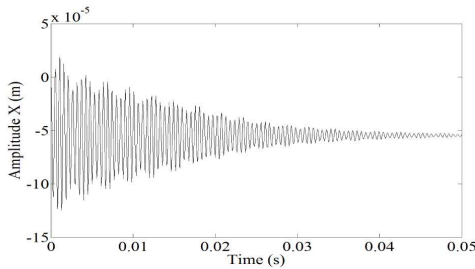
of shoe lining, back-plate stiffness, torque generated when brake applied, normal contact force, arc angle of the brake shoes and also the stiffness of the drum. The change of location of center of pressure on the drum will affect the diametral modes of the system, which will also influence the stability of the system [23].

Normal load, $N=5000$ N



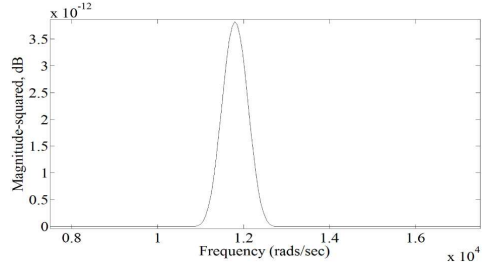
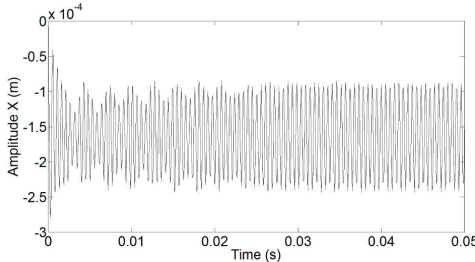
11790 rad s⁻¹; 14060 rad s⁻¹

Normal load, $N=10000$ N



11790 rad s⁻¹

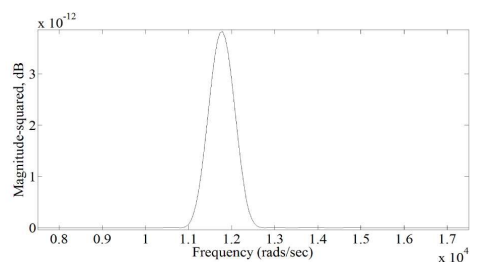
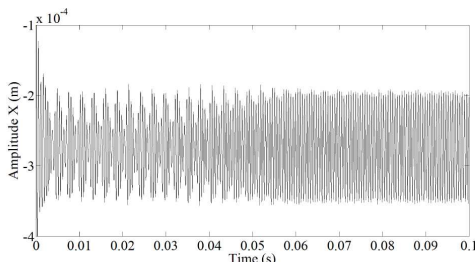
Normal load, $N=15000$ N



11790 rad s⁻¹

Limit cycle: 0.140 mm

Normal load, $N=25000$ N

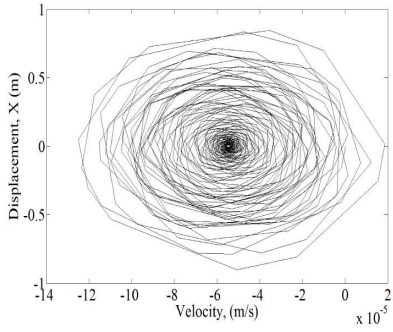


11790 rad s⁻¹

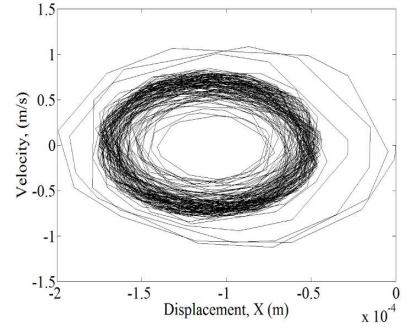
Limit cycle: 0.160mm

Fig. 6. Time series and frequency responses for various values of normal load

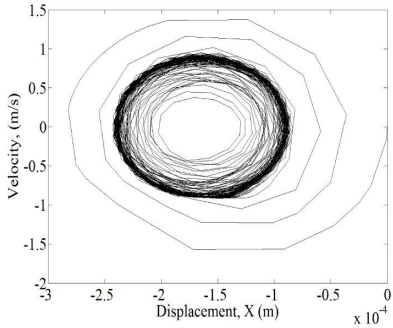
Normal load, $N=5000$ N



Normal load, $N=10000$ N



Normal load, $N=15000$ N



Normal load, $N=25000$ N

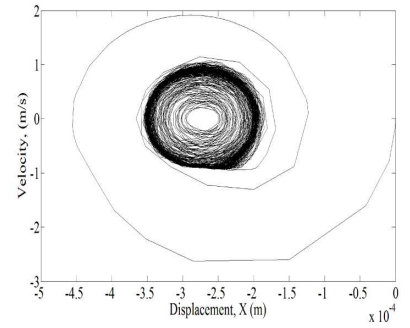
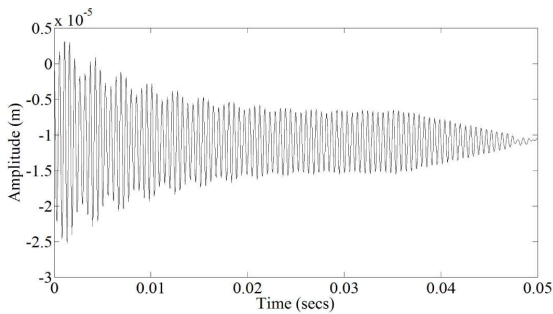
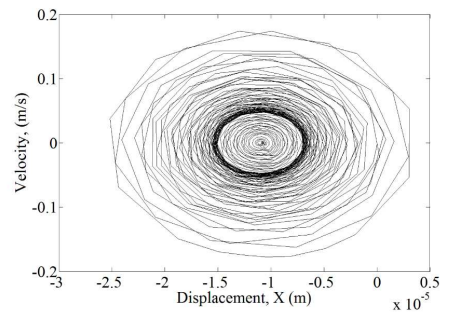


Fig. 7. Phase-plane for various values of normal load

Time Series



Phase-plane



Frequency response

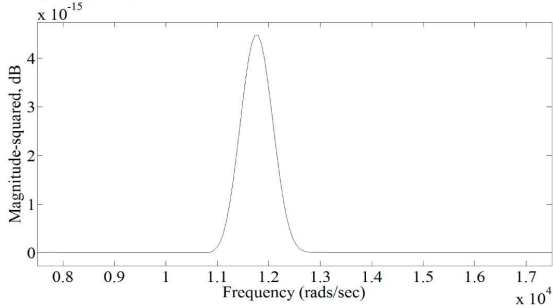


Fig. 8. Time series and frequency responses for various values of speed

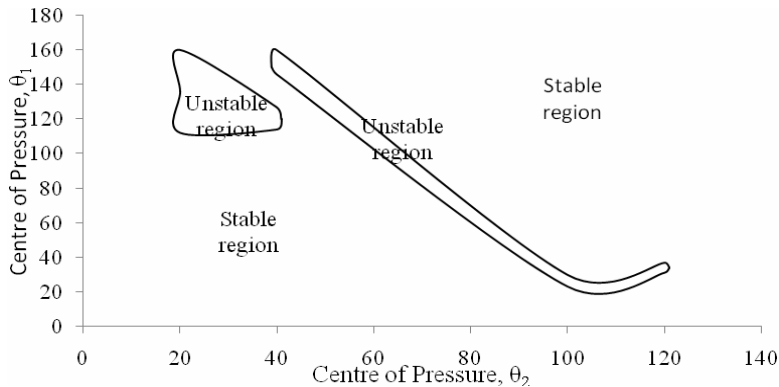


Fig. 9. Effect of centre of pressure on drum

Conclusions

1. The binary flutter instability is excited by the increase of friction coefficient. Meanwhile the negative friction-velocity instability mechanism is excited with the increase of normal load or decrease of the sliding velocity. The binary flutter instability mechanism had been excited when the value of friction coefficient is more than 0.40.
2. The negative friction-velocity instability mechanism had been excited when the normal load increases up to 15 kN or the sliding velocity reduces from 0.12 m s⁻¹ to 0.05 m s⁻¹.

Acknowledgements

This paper is done with the financial support from USM fellowship, research grants A/C 6071160 and A/C 6035243. The authors would like to thank Ms Ko Ying Hao for her assistance.

References

- [1] Huang J., Krousgrill C. M., Bajaj A. K. "Modelling of automotive drum brake for squeal and parameter sensitivity analysis", *Journal of Sound and Vibration*, **289**, 245-263 (2006).
- [2] Day A. J. "An analysis of speed, temperature, and performance characteristics of automotive drum brakes", *Journal of Tribology*, **110**, 298-305 (1988).
- [3] Liu P., Zheng H., Cai C., Wang Y. Y., Lu C., Ang K. H., Liu G. R. "Analysis of disc brake squeal using the complex eigenvalue method", *Applied Acoustics*, **68**, 603-615 (2007).
- [4] Hulten J. "Some drum brake squeal mechanisms", *SAE 951208* (1995).
- [5] Paliwal M., Mahajanb A., Donb J., Chub T., Noiseand P.F. "Vibration analysis of a disc brake system using a stick-slip friction model involving coupling stiffness", *Journal of Sound and Vibration*, **282**, 1273-1284 (2005).
- [6] Kinkaid N. M., O'Reilly O. M., Papadopoulos P. "On the transient dynamics of a multi-degree-of-freedom friction oscillator: a new mechanism for disc brake noise", *Journal of Sound and Vibration*, **287**, 901-917 (2005).
- [7] Zhou M., Wang Y., Huang Q. "Study on the stability of drum brake non-linear low frequency vibration model", *Arch Appl. Mech.*, **77**, 473-483 (2007).
- [8] Lee J. M., Yoo S. W., Kim J. H., Ahn C. G. "A study on the squeal of a drum brake which has shoes of non-uniform cross-section", *Journal of Sound and Vibration*, **240**(5), 789-808 (2001).
- [9] Chen G. X., Zhou Z. R. "Correlation of a negative friction-velocity slope with squeal generation under reciprocating sliding conditions", *Wear*, **255**, 376-384 (2003).
- [10] Gianninia O., Akayb A., Massia F., "Experimental analysis of brake squeal noise on a laboratory brake setup", *Journal of Sound and Vibration*, **292**, 1-20 (2006).

- [11] **Gianninia O., Sestieri A.** "Predictive model of squeal noise occurring on a laboratory brake", *Journal of Sound and Vibration*, **296**, 583-601 (2006).
- [12] **Gianninia O., Massib F.** "Characterization of the high-frequency squeal on a laboratory brake setup", *Journal of Sound and Vibration*, **310**, 394-408 (2008).
- [13] **Shin K., Brennan M. J., Oh J. -E., Harris C. J.** "Analysis of disk brake noise using a two-degree-of-freedom model", *Journal of Sound and Vibration*, **254**(5), 837-848 (2002).
- [14] **Kanga J., Krougrilla C. M., Sadeghia F.** "Comprehensive stability analysis of disc brake vibrations including gyroscopic, negative friction slope and mode-coupling mechanisms", *Journal of Sound and Vibration*, **324**, 387-407 (2009).
- [15] **Hoffmann N., Gaul L.** "Effects of damping on mode-coupling instability in friction induced oscillations", *Z. Angew. Math. Mech.*, **83**(8), 524-534 (2003).
- [16] **Hoffmann N., Wagner N., Gaul L.** "Quenching mode-coupling friction-induced instability using high-frequency dither", *Journal of Sound and Vibration*, **279**, 471-480 (2005).
- [17] **Guan D., Huang J.** "The method of feed-in energy on disc brake squeal", *Journal of Sound and Vibration*, **261**, 297-307 (2003).
- [18] **Haverkamp M., Koopmann N.** "Acoustic quality control of drum brake shoes", *Joint Congress CFA/DAGA '04*, Strasbourg, France, 22-25 March 2004.
- [19] **Liles G. D.** "Analysis of disc brake squeal using finite element methods", SAE 891150 (1989).
- [20] **Mohd. Ripin Z.** "Analysis of disc brake squeal using the finite element method", PhD Thesis, University of Leeds (1995).
- [21] **Okamura H., Nishiwaki M.** "A study on brake noise (drum brake squeal)", *JSME International Journal*, Series 3, **32**(2), 206-214 (1989).
- [22] **Hoffmann N., Fischer M., Allgaier R., Gaul L.** "A minimal model for studying properties of the mode-coupling type instability in friction induced oscillations", *Mechanics Research Communications*, **29**, 197-205 (2002).
- [23] **Ioannidis P., Brooks P. C., Barton D. C.**, "Drum brake contact analysis and its influence on squeal noise prediction", *SAE 2003-01-3348* (2003).
- [24] **Guan D., Jiang D.** "A study on disc brake squeal using finite element methods", SAE 980597 (1998).
- [25] **Ouyang H., Mottershead J. E., Cartmell M. P., Friswell M. I.** "Friction-induced parametric resonances in disc: effect of a negative friction-velocity relationship". *Journal of Sound and Vibration*, **209**(2), 251-264 (1998).
- [26] **Capone G., D'Agostino V., Valle S. D., Guida D.** "Influence of the vibration between static and kinetic friction on stick-slip instability", *Wear*, **161**, 121-126 (1992).
- [27] **Hoffmann N., Bieser S., Gaul L.** "Harmonic balance and averaging techniques for stick-slip limit-cycle determination in mode-coupling friction self-excited systems", *Technische Mechanik*, band **24**, Heft 3-4, 185-197 (2004).
- [28] **Von Wagner U., Hochlenert D., Hagedorn P.** "Minimal models for disc brake squeal", *Journal of Sound and Vibration*, **302**, 527-539 (2007).
- [29] **Hashemi-Dehkordi S. M., Mailah M., Abu-Bakar A. R.** "A Robust Active Control Method to reduce brake noise", *International Conference on Robotics and Biomimetics*, Bangkok, 2009.
- [30] **Bogacki P., Shampine L.F.** "A 3(2) pair of Runge - Kutta formulas", *Applied Mathematics Letters*, **2**(4), 321-325 (1989).
- [31] **Felske A., Hoppe G., Matthai H.** "A study on drum brake noise by holographic vibration analysis", SAE800222 (1980).